DOI: 10.13009/EUCASS2017-521

Monte Carlo analysis of a LEO reentry mission by solid rocket propulsion

F. Maggi⋆†*, C. Paravan*⋆*, M. Benetti*⋆*, M. Benetti*⋆*, R. Bisin*⋆*, and T. Shimizu*⋆
⋆*Dept. Aerospace Science and Technology, Politecnico di Milano*
Via La Masa 34, Milan, 20156, Italy
filippo.maggi@polimi.it · christian.paravan@polimi.it · michele.benetti@mail.polimi.it ·
mose.benetti@mail.polimi.it · riccardo.bisin@mail.polimi.it ·
tomohiro.shimitzu@mail.polimi.it
†Corresponding author

Abstract

Deorbiting missions by means of a solid rocket motor represent a viable solution to implement mitigation actions against the proliferation of new debris population. This specific technology is flight-proven, simple to implement, and fits the main performance requirements for the mission (particle-free exhaust gases, readiness, specific impulse) but it lacks of operational flexibility. The present work considers the scenario of a hypothetical industrial product for deorbiting purposes, tuned on a reference satellite weighing 700 kg in LEO, and used in different off-design scenarios. In the present paper the example of mission accomplishment analysis as a function of two parameters (such as initial altitude or rocket propellant mass) are quantified using a Monte Carlo analysis. Mission feasibility and flight path angle at atmospheric reentry are monitored and discussed. The methodology presented in the paper is general and can be extended to assess the influence of more parameters, generating a realistic evaluation scenario. The work is not related to existing or currently planned industrial projects or companies.

Nomenclature

Acronyms

COTS commercial off the shelf

MC Monte Carlo

MR mass ratio

Greek symbols

α coverage probability

$\Delta\cdot$ variation of a parameter

ϵ confidence half-interval, relative value

γ Flight path angle

μ average value

σ standard deviation

Roman symbols

d confidence half-interval, absolute value

e eccentricity

g_0 standard gravity, $9.81\,\mathrm{m\,s^{-2}}$

I impulse

M mass

N number of samples

R orbital radius

T temperature

V orbital velocity

Z standardized normal random variable

Subscripts and superscripts

$\bar{\cdot}$ statistical estimator of a variable

0 initial condition

apo apogee

atm ref. to atmospheric reentry

c ref. combustion chamber

circ circular orbit

f final condition

DOI: 10.13009/EUCASS2017-521

mol	molar
p	propellant
per	perigee
safe	safe condition
vac	vacuum conditions

1. Introduction

The future sustainability of space activities in LEO requires the implementation of reliable end-of-life disposal maneuvers on present and future satellites. The forecasts for abandoned objects of in-orbit population are casting shadows on the long-term survivability of spacecrafts, as the number-density of the items is increasingly growing due to the Kessler syndrome.[1–3] This runaway effect, fed by both fragmentation of existing bodies and introduction of new junk items, is now uncontrolled. According to evolutionary models based on collision statistics, in a long-term perspective remediation activities (debris active removal) are necessary for the stabilization of the environment. These mission concepts are complex and very often the TRL of enabling sub-parts (approaching, recognition, de-tumbling, docking, disposal) do not allow an early practical implementation. Examples of such scenarios are widely explored in the competent literature and a complete review is quite impossible. A couple of examples are given in papers by Castronuovo and DeLuca *et al.*[4,5] The evolutionary models also suggest that mitigation actions (implementation of proper end-of-life strategy on new spacecrafts) do not suffice for the stabilization of the in-orbit population but they can limit the growth of the object spatial density.[6] Proper disposal maneuvers can be implemented using existing on-board systems or specific deorbiting devices. In most of the cases, the sub-components of such missions are COTS systems or require minor developments for the specific application.

In-orbit disposal can be performed by natural orbit decay and atmospheric capture, targeted reentry, or re-orbiting to graveyard orbits.[7] The choice of the specific activity depends on different factors or risks. Natural orbit decay is considered for such spacecrafts that for which the ground casualty at reentry is lower than 1 over 10000, on the basis of component survivability at re-entry.[8] Mass, materials, presence of specific high-strength components are some of the factors which determine which strategy can be adopted. According to data reported in a paper by Heinrich and co-authors, preliminary ESA estimates suggest that satellites having mass larger than 500 kg already do not comply with the ground casualty risk limit.[9] In this latter case, targeted re-entry or repositioning on a graveyard heliocentric orbit are requested.

Chemical rocket systems seem to represent the only propulsion suitable for commanded deobiting of massive satellites that require targeted reentry. In general, this kind of maneuver requires an accurate and relatively high-thrust firing in a short time, as the spacecraft should impact the atmosphere with a defined flight path angle for better ground footprint determination. Electric propulsion devices supply high specific impulse but the low thrust level confines its application only to uncontrolled reentry missions. In a paper by Janovski *et al.* published in 2003, an analysis of different deorbiting missions on various satellites and propulsion devices was accomplished.[7] As a conclusion, the authors stated that the best option, at the date of the paper, was represented by the solid propulsion, followed by the monopropelants. Hybrid rockets were discarded for low TRL. The solid rocket motor technology grants reliability, compactness, low structural mass index, storability (yet, to be proven under long-term space conditions), readiness, and low cost. The low level of specific impulse, in comparison to other technologies, does not represent a consistent penalty, as the ΔV requirements are quite small. On the other hand, the lack of run-time flexibility reprsents a technological limit (e.g. no throttling capability or combustion cut/reinition posibility). The optimal choice of a solid propellant motor is valid if the rocket can be tailored on the specific mission but this solution becomes unfeasible from an industrial viewpoint. In this respect, it is more convenient to explore the posibility of producing a standard rocket motor which can fit most of the potential missions, as single item or in a multiple configuration, even with a sub-optimal mission.

The present work considers the scenario of a hypothetical industrial product for deorbiting purposes. One model of solid rocket motor is developed for a reference satellite weighting 700 kg which has to impact the atmosphere with a flight path angle $\gamma = 2°$. After the evaluation of a preferential propellant mass budget, the influence of initial orbiting altitude and of propellant mass uncertainty on mission accomplishment are quantified using a Monte Carlo analysis. The flight path angle at atmospheric reentry is monitored and discussed.

2. Selection of the ΔV

In this paper the authors are considering a single rocket motor granting the reentry maneuver of a satellite having a mass of 700 kg and placed in a circular orbit in the altitude range 400 km to 1600 km. As an optimal choice, the spacecraft should impact the atmosphere, placed at the reference altitude of 150 km, with a flight path angle $\gamma_{atm} = 2°$.

DOI: 10.13009/EUCASS2017-521

For simplicity, the same maneuver strategy is assumed at all the other altitudes, using an impulsive firing with a steady-state thrust profile. An elliptical orbit transfer is considered and point-wise modeling is assumed for the dynamics.

The designed rocket is capable of accomplishing the optimal deorbiting maneuver only from one specific initial orbit whereas a sub-optimal reentry attitude is obtained for the rest of the altitudes. Every initial satellite condition has only one elliptical transfer orbit granting $\gamma_{atm} = 2°$, which corresponds to one unique ΔV requirement. Due to intrinsic limitation of solid rocket motor technology, it is possible to assume that the ΔV supplied is defined at the design phase and cannot be regulated. It follows that, once the rocket is produced, only one initial altitude grants the deorbiting mission accomplished with the optimal reentry angle. For the other cases, if the satellite is orbiting at an altitude lower than the design condition, the ΔV the eccentricity of the resulting transfer orbit is larger than expected, with the perigee getting closer to the trajectory focus. The intersection with the atmosphere is guaranteed but the angle is higher than expected. When the satellite altitude is higher than the design selection, the supplied ΔV is lower than requested, moving the perigee of the transfer orbit farther from the focus. In this simplified framework a reentry mission is considered to fail when no intersection is obtained between the transfer orbit and the 150 km altitude level. The limiting condition corresponds to a flyby with $\gamma_{atm} = 0°$, as represented in Fig. 1.

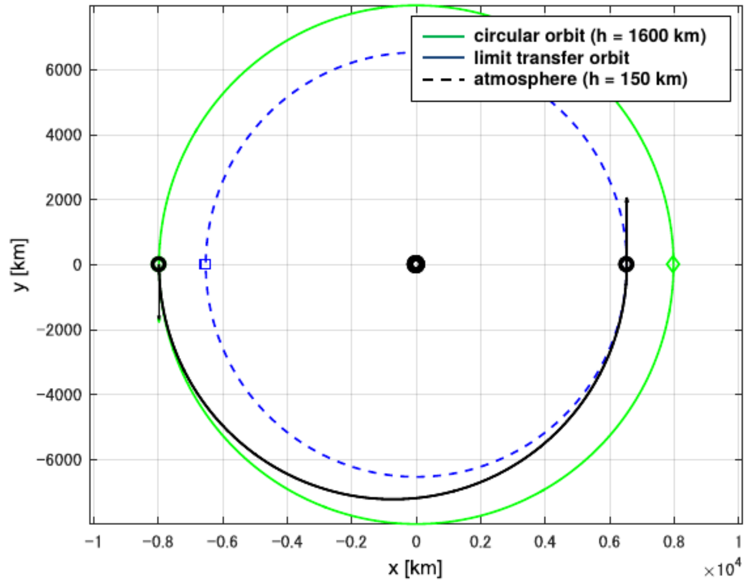

Figure 1: Reentry maneuver. Limiting orbit condition granting $\gamma = 0°$.

As a design choice, the rocket should be capable of reentering all the satellites having mass of 700 kg in the requested altitude range 400 km to 1600 km. A success/failure map has ben produced to support the selection of the propellant mass budget (Fig. 2). The color map identifies the value of γ_{atm} for varying ΔV and initial altitude. The blank region corresponds to the locus of missed reentry maneuvers ($\gamma_{atm} < 0$).

The results show that the probability of missed reentries grows for higher orbits. The value of $\Delta V_{safe} = 362\,\mathrm{m\,s^{-1}}$ is the minimum which ensures the mission accomplishment for the entire altitude range. The resulting rocket engine is the optimal choice for the altitude of 1538 km, granting $\gamma_{atm} = 2°$. For the altitude of 1600 km it grants the limit condition of $\gamma = 0°$ whereas the spacecrafts located below the level of 1538 km will impact the atmosphere with $\gamma > 2°$. The design orbit transfer for deorbiting has the following properties:

- $R_{apo} = 7916\,\mathrm{km}$
- $R_{per} = 6483\,\mathrm{km}$
- $e = 0.0995$
- $V_{atm} = 8.17\,\mathrm{km\,s^{-1}}$

3. Propellant selection

The propellant considered for this mission is a standard AP/HTPB composition. This selection grants the benefits from being relatively cheap, with good aging property and good performances in terms of burning rate and specific

DOI: 10.13009/EUCASS2017-521

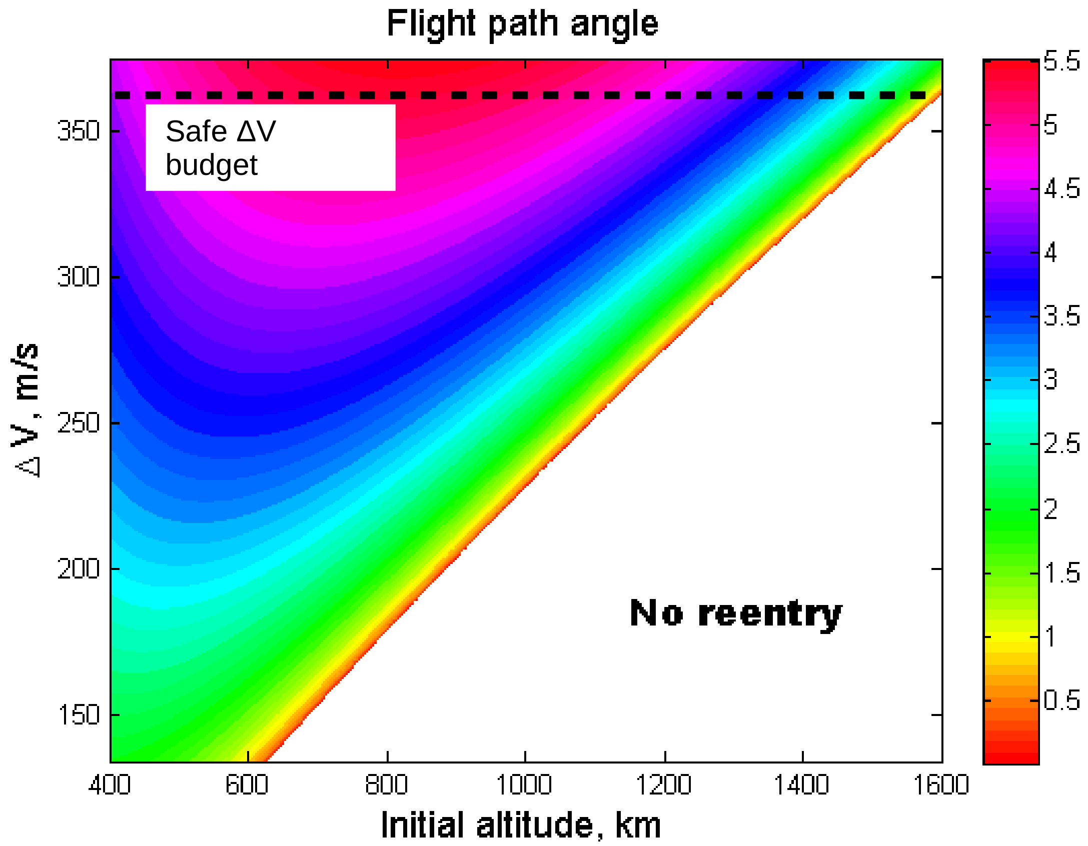

Figure 2: Success map for different ΔV and altitude levels. Color map: γ.

DOI: 10.13009/EUCASS2017-521

impulse. In principle, this formulation produces a plume free from solid residues, which is one of the requirements of the ESA compliance guidelines for deorbiting operations.[10] A reference AP/HTPB composition having an 80/20 mass fraction was considered. The performance of this propellant was obtained through the NASA CEA thermochemical code, considering a chamber pressure of 70 bar and an area ratio of 100, with vacuum discharge under frozen expansion model.[11] Data are reported in Table 1. The Tsiolkovsky equation for drag-free and gravity-free maneuvers enables the computation of the mass ratio of the spacecraft (rocket and satellite), being $\exp(\Delta V/(I_s\, g_0)) = 1/MR = M_0/M_f$. Once a structural mass index is set to 10% for the solid propulsion unit, a propellant mass M_p = 104.6 kg was derived.

Table 1: Performance of the AP/HTPB propellant

T_c, K	2343
M_{mol-c}, g mol^{-1}	22.1
I_{s-vac}, s	268

4. Off-design sensitivity analysis

The derived rocket motor is now evaluated as a deorbiting device under non-nominal conditions using a Monte Carlo approach. In this work the analysis is limited to the variability of the initial deorbiting altitude and the propellant loaded in the rocket motor. However, this general methodology can be applied to different types of aleatory or epistemic mission uncertainties.[12,13] A uniform probability distribution is used to sample the initial deorbiting altitude within the range 400 km to 1600 km, as no preferential value is defined. The variation over the propellant mass is an aleatory source of uncertainty because it is representative of a deviation from the nominal value (e.g. production variability, combustion slivers, ...). For this reason it is modeled as a Gaussian distribution of items around the nominal value. The associated uncertainty is set here to 2 % (with 95% confidence level). As a result, the flight path angle at the impact with the atmosphere is monitored. Examples of generated populations for M_p and for altitude are given in Fig. 3 and Fig. 4, respectively.

4.1 Variation of γ_{atm} due to change of initial deorbiting altitude

This case study mapped γ_{atm} for spacecrafts initially orbiting at different initial altitudes. Thanks to selection criterion implemented in Sec. 2, none of the runs brings to a failed reentry. The frequency diagram, reported in Fig. 5, shows that the obtained angles span from zero to about 5.5°. In most of the cases the flight path angle is larger than for the design condition, with a maximum on the last bin of the frequency plot. This result is expected as the rocket is optimized for the deorbiting of a satellite placed at the altitude of 1538 km.

4.2 Variation of γ_{atm} due to change of M_p

The impact on γ_{atm} of the propellant mass loaded in the deorbiting rocket is monitored. The sample population is produced by sampling a Gaussian distribution and causes a variation of the delivered ΔV. Figure 6 presents a parametric evaluation over four different initial orbit altitudes. The declared uncertainty of 2 % over the nominal propellant mass does not generate a great variation in the expected flight path angle for those trajectories that deorbit from low altitude. In the reported figures, spacecrafts at 400 km and at 800 km altitude feature a nearly symmetric distribution of γ_{atm} and the span is lower than 1°. The result is justified by the fact that the ΔV of the rocket motor is oversized for the mission. If a spacecraft at the deorbiting altitude of 1538 km is condsidered, the resulting distribution of γ_{atm} is located around the nominal reentry flight path angle of 2° but the span increases. Failure cases are not yet detected. When the limit case of a satellite orbiting at 1600 km is considered, the span of the distribution becomes larger than 2° approaching the failure limit of $\gamma_{atm} = 0°$.

4.3 Variation of γ_{atm} due to change of M_p and initial altitude

The variation of loaded propellant mass and initial altitude are now overlapped. The respective populations are sampled from a uniform probability for the altitude and a Gaussian distribution for the propellant content. The evaluation of the confidence level reached by the method was based on the estimated statistical properties of γ_{atm} average value, using

DOI: 10.13009/EUCASS2017-521

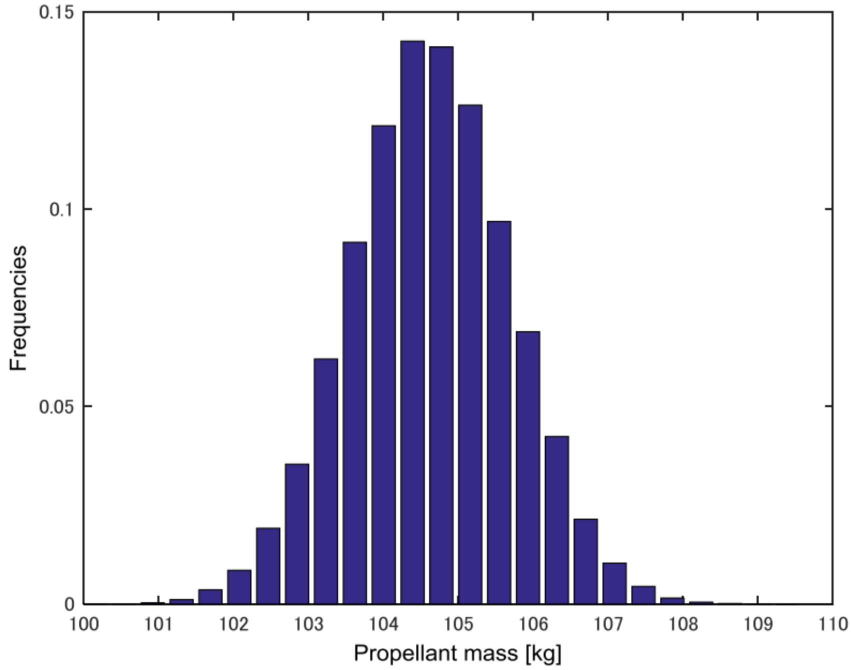

Figure 3: Population generated for M_p. Gaussian distribution with 2% uncertainty, 100000 samples.

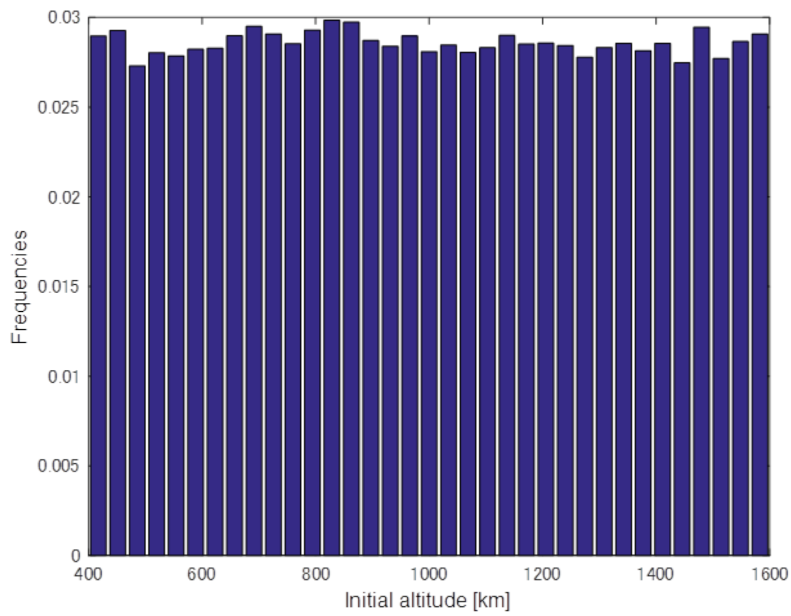

Figure 4: Population for altitude. Uniform distribution, 100000 samples.

DOI: 10.13009/EUCASS2017-521

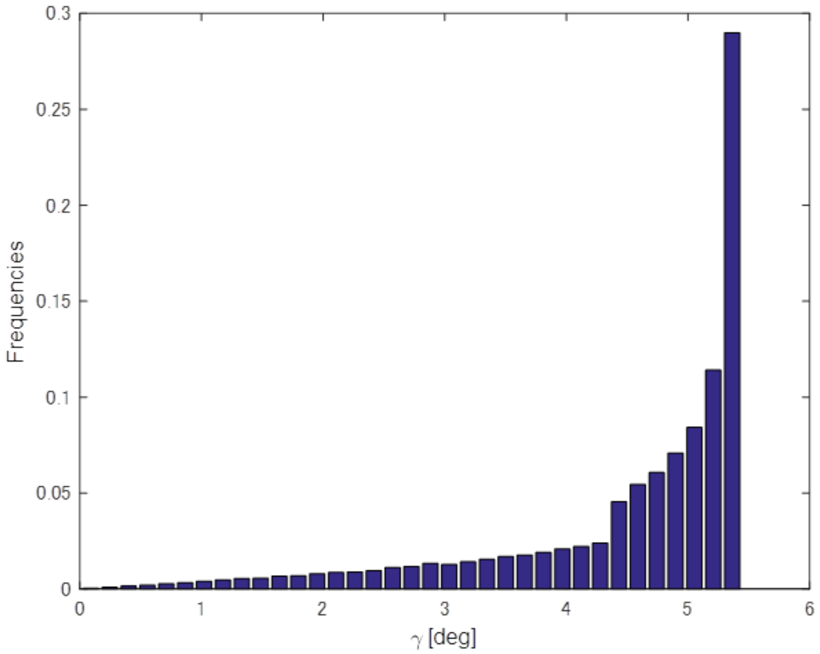

Figure 5: Population of γ_{atm} obtained by changing the initial deorbiting altitude

Table 2: Correlation between MC accuracy and sample number, based on statistical estimators

No. samples	$\bar{\mu}_\gamma$	$\bar{\sigma}_\gamma$	$N_{2\%}$	$N_{1\%}$	$N_{0.5\%}$
1000	4.593	1.0168	470	1883	7531
2000	4.521	1.0926	556	2224	8896
5000	4.539	1.0593	523	2092	8368
7000	4.522	1.0775	545	2180	8848

the principle of the sequential stopping rule.[14] In Table 2 the number of samples requested to obtain a relative error half-interval $\epsilon = 2\%$, 1%, and 0.5% are computed, according to Eq. 1.

$$N_\epsilon = \left(\frac{\bar{\sigma}_N Z_\alpha}{d}\right)^2 \tag{1}$$

The symbols ϵ and d represent the confidence half-interval, respectively in percent or in absolute value, σ_N is the estimator of the standard deviation, Z_α is the standardized normal random variable for a coverage probability of α ($Z = 1.96$ for a number large enough of samples and for a 95% confidence level). As a trade-off between accuracy and computational cost, the number of items was reduced to 5000 samples per each generated population. This choice ensures a confidence level between 0.5% and 1%, evaluated on the monitored variable.

In the distribution reported in Fig. 7 the highest frequency number is located beyond $\gamma = 5°$, even though the peak is not placed at the edge of the orbit range. The majority of the satellites enter the atmosphere with a flight path angle larger than the optimal value of 2°. Some missions are not successful as the propellant mass budget is not sufficient. A failure map is reported in Fig. 8, as a function of initial spacecraft altitude and M_p. A line splits the successful from the unsuccessful cases. The number of failures is sensitive to the uncertainty over M_p, as the available ΔV is dependent from it. Table 3 reports the probability of missed reentry missions when the confidence interval on the propellant load is varied from 1 to 3 %. The resulting rate of missed reentry maneuvers grows but the trend is less-than-linear and the value remains below 1 %.

5. Conclusion

A reference satellite having 700 kg mass was considered for a deorbiting mission from a circular orbit. As a possible commercial scenario, the rocket motor was designed to perform the mission for a wide population of satellites orbiting

DOI: 10.13009/EUCASS2017-521

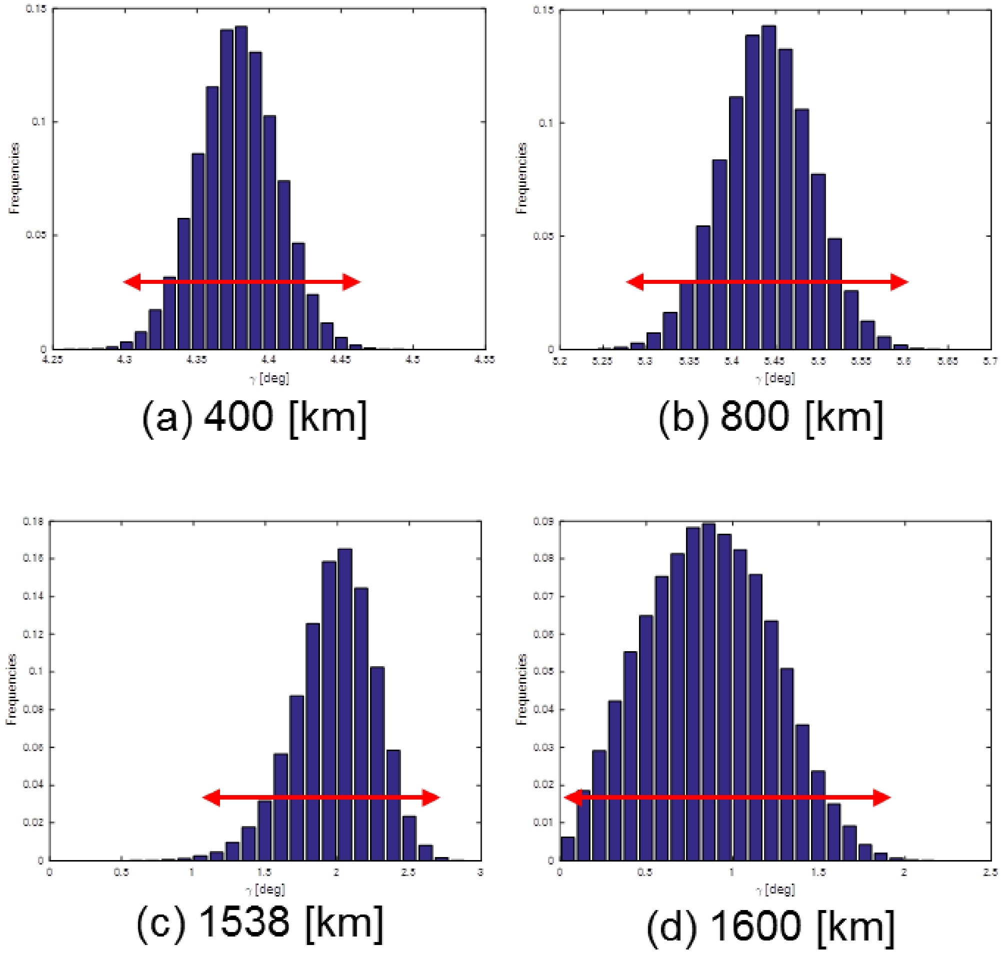

Figure 6: Variation of γ_{atm} following the changes of propellant mass

ϵ_{Mp}, %	Failure, %
1.0	0.298 %
2.0	0.555 %
3.0	0.767 %

Table 3: Probability of missed reentry missions. Uncertainty of M_p is varied. N = 5000.

DOI: 10.13009/EUCASS2017-521

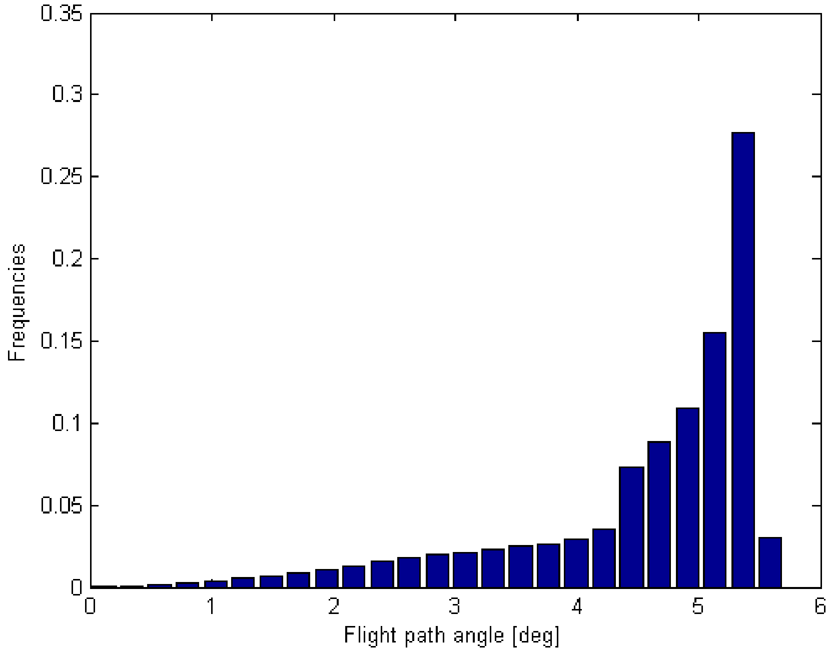

Figure 7: Population of γ_{atm} after altitude and M_p variation.

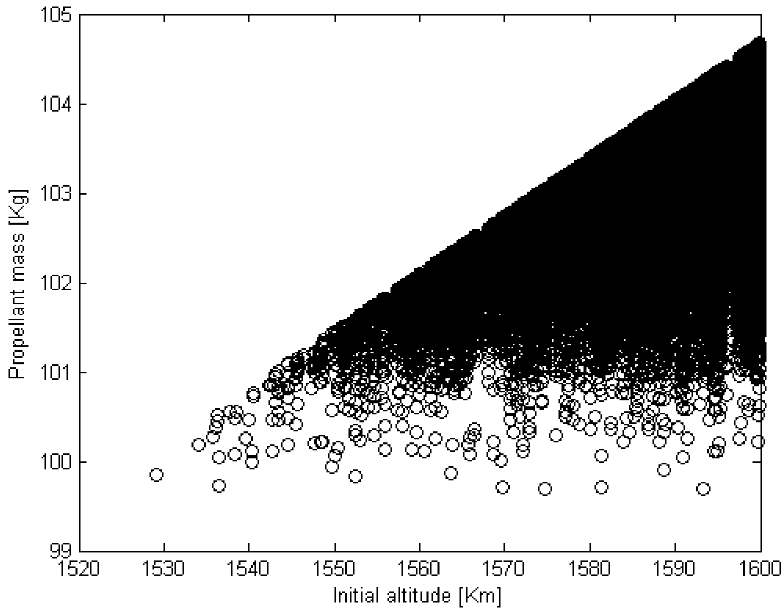

Figure 8: Failure map based on variabiliy of altitude and M_p).

DOI: 10.13009/EUCASS2017-521

at different altitudes. In the present paper this range was arbitrarily fixed to 400 km to 1600 km. An optimal rocket motor featured by minimum propellant mass was defined and the deorbiting capability was evaluated, introducing uncertainty sources on initial altitude and loaded propellant mass. Results demonstrated that the probability of mission failure is below 1 % within the selected boundaries of 3% propellant mass uncertainty. However, in most of the cases the flight path angle at the atmospheric reentry was larger than the design one.

The present paper has shown a quick evaluation methodology for design and off-design considerations about deorbiting missions. The extension to further uncertainty sources (i.e. mass of the spacecraft) is of paramount importance for more realistic predictions. From the algorithm viewpoint, the increment of one or more dimensions in the variable space does not pose peculiar problems. However, the computational cost may become soon prohibitive. In this respect, more efficient sampling techniques may be implemented (e.g. Latin Hypercubes). In addition, MC algorithms are prone to parallelization with both shared and distributed memory paradigms, contributing to the reduction of the wall-clock time.

References

[1] D. J. Kessler, N. L. Johnson, J-C Liou, and M. Matney. The Kessler syndrome: implications to future space operations. *Advances in the Astronautical Sciences*, 137(8):2010, 2010.

[2] J-C Liou. Collision activities in the future orbital debris environment. *Advances in Space Research*, 38(9):2102–2106, 2006.

[3] J-C Liou and N. L. Johnson. Instability of the present leo satellite populations. *Advances in Space Research*, 41(7):1046–1053, 2008.

[4] M. M. Castronuovo. Active space debris removal: A preliminary mission analysis and design. *Acta Astronautica*, 69(9):848–859, 2011.

[5] L.T. DeLuca, F. Bernelli, F. Maggi, P. Tadini, C. Pardini, L. Anselmo, M. Grassi, D. Pavarin, A. Francesconi, F. Branz, S. Chiesa, N. Viola, C. Bonnal, V. Trushlyakov, and I. Belokonov. Active space debris removal by a hybrid propulsion module. *Acta Astronautica*, 91:20–33, 2013.

[6] J-C Liou, N. L. Johnson, and N. M. Hill. Controlling the growth of future leo debris populations with active debris removal. *Acta Astronautica*, 66(5):648–653, 2010.

[7] R. Janovsky. End-of-life de-orbiting strategies for satellites. In *54th International Astronautical Congress*, number IAC-03-IAA.5.4.05, pages IAA–5, 2002.

[8] Anon. Space debris mitigation policy for agency projects. ESA/ADMIN/IPOL(2014)2, 2014.

[9] S. Heinrich, F. Leglise, L. Harrison, F. Renard, and O. Nold. Trade-off atmospheric re-entry: Design for demise vs controlled re-entry. In Tommaso Sgobba and Isabelle Rongier, editors, *Space Safety is No Accident: The 7th IAASS Conference*, pages 423–435. Springer International Publishing, 2015.

[10] Anon. ESA space debris mitigation compliance verification guidelines. ESSB-HB-U-002 Issue 1, 2015.

[11] S. Gordon and B. S. McBride. Computer program for calculation of complex chemical equilibrium compositions and applications. Technical Report RP-1311, NASA Reference Publication, 1994.

[12] C. J. Roy and W. L. Oberkampf. A comprehensive framework for verification, validation, and uncertainty quantification in scientific computing. *Computer Methods in Applied Mechanics and Engineering*, 200(25):2131 – 2144, 2011.

[13] W. L. Oberkampf, S. M. DeLand, B. M. Rutherford, K. V. Diegert, and K. F. Alvin. Error and uncertainty in modeling and simulation. *Reliability Engineering & System Safety*, 75(3):333 – 357, 2002.

[14] M. J. Gilman. A brief survey of stopping rules in monte carlo simulations. In *Proceedings of the Second Conference on Applications of Simulations*, pages 16–20, 1968.